Int. J. Heat Mass Transfer. Vol. 22, pp. 1221–1229
Pergamon Press Ltd. 1979. Printed in Great Britain

THE ACCURACY AND RESOLVING POWER OF ONE DIMENSIONAL TRANSIENT INVERSE HEAT CONDUCTION THEORY AS APPLIED TO DISCRETE AND INACCURATE MEASUREMENTS

R. G. HILLS and G. P. MULHOLLAND
Department of Mechanical Engineering, New Mexico State University, Las Cruces, N.M., U.S.A.

(*Received* 12 *June* 1978 *and in revised form* 15 *February* 1979)

Abstract—The inverse heat conduction problem is defined as one for which interior conditions are prescribed and the desired quantity is a surface condition. In the present work, the surface temperature histories for an infinite slab are evaluated using discrete and inaccurate internal measurements. The method of Backus and Gilbert is used to determine the resolving power of the measurements and the accuracy of the resulting surface temperature predictions. The trade-offs that exist between resolving power and accuracy are illustrated.

NOMENCLATURE

- $\bar{\mathbf{A}}$, kernel matrix, equation (22);
- $\mathbf{a}$, vector of coefficients a_i, equation (45);
- $\bar{\mathbf{B}}$, pseudoinverse of $\bar{\mathbf{A}}$;
- D, integration weighting function, equation (36);
- $\bar{\mathbf{E}}$, error matrix (covariance matrix), equation (45);
- $\bar{\mathbf{I}}$, identity matrix;
- K, integrating kernel, equation (14);
- L, width of slab;
- N, number of measurements;
- $\bar{\mathbf{S}}$, spread matrix, equation (48);
- s, spread;
- T, temperature;
- T_s, surface temperature;
- $\mathbf{T}_s$, vector of surface temperatures;
- $\hat{T}_s$, estimate of surface temperature;
- $\hat{\mathbf{T}}$, estimate of surface temperature vector $\mathbf{T}_s$;
- t, dimensionless time;
- t^*, time;
- V, solution to supplementary problem, equations (8) and (9);
- $\bar{\mathbf{W}}$, $N \times N$ matrix;
- w, parameter;
- x, dimensionless spatial position;
- x^*, spatial position.

Greek symbols

- α, thermal diffusivity;
- β, parameter;
- β_n, eigenvalue;
- $\boldsymbol{\gamma}$, vector of measurements γ_i;
- $\Delta\hat{T}_s$, estimated error in the prediction T_s;
- $\Delta\boldsymbol{\gamma}$, vector of measurement errors;
- ε, error.

INTRODUCTION

THE DIRECT problem in transient heat conduction theory involves the evaluation of the interior conditions of a region from the boundary and initial conditions of that region. A corresponding inverse problem involves the evaluation of a boundary condition from the remaining boundary and initial conditions and some interior condition. An important characteristic of inverse heat conduction theory is well illustrated by a quotation from Stolz [1]:

> "In a heat-conduction system the effect of boundary conditions is always damped at interior points, and the inverse problem involves basically the extrapolation of the damped datum to the surface..."

In the direct problem of heat conduction, the higher frequency components of the boundary conditions will be damped at a higher rate than the lower frequency components, whereas in the inverse problem, the higher frequency components of the internal measurements will be selectively amplified as the measurements are projected to the surface. Thus, any noise in the measurements will be amplified in the projection to the surface and the resulting surface condition predictions might be overwhelmed by the noise of the interior measurements.

A second problem that arises in inverse conduction theory is the question of the uniqueness of the surface condition histories as predicted by discrete internal measurements. One cannot hope to find a unique surface temperature history using only interior temperature measurements made at discrete times. There will be an infinity of surface temperature histories that will satisfy a finite set of discrete internal measurements, and the surface conditions will only be resolvable to within certain limits. The consideration of the above problems when utilizing inverse theory in conjunction with discrete experimental data is a necessary part of the analysis.

Many techniques have been presented to handle inverse problems in heat conduction theory. The techniques include graphical methods [2], finite difference and finite element methods [3–7], polynomial methods [8–12], and exact methods [1, 13–19]. The evaluation of thermal properties and temperature responses from thermocouple measure-

ments has also received attention [12, 20–24]. In geophysics, methods of handling inverse problems are well established. Since geophysicists often deal with discrete and inaccurate data in making inferences about the earth, it is natural that some of their methods can be adapted for use in the inverse heat conduction area. One such method is that of Backus and Gilbert [25] who have developed an elegant method for quantitatively evaluating the resolving power (a measure of uniqueness) and accuracy of predictions from discrete and inaccurate methods.

The purpose of this work is to adapt Backus–Gilbert inverse theory to the predictions of surface temperature histories of an infinite slab given an insulated second surface condition and temperatures at some interior point that are known to within some error at given discrete times. Comparisons between actual and predicted results, and trade-offs between resolving power and accuracy are illustrated.

ANALYSIS

Reduction of the problem to appropriate form

Consider an infinite slab (see Fig. 1) with constant thermal properties in which the temperature distribution is a function of position x^* and time t^*. Let

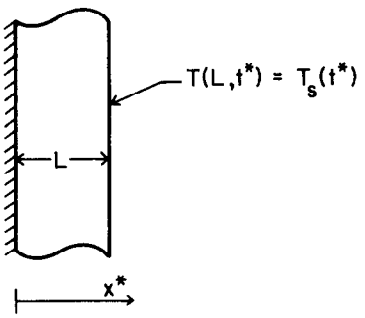

FIG. 1. Geometry of the problem.

one side of the slab, $x^* = 0$, be insulated while the second side, $x^* = L$, be at an unknown temperature which varies with time. If the slab's initial temperature is zero, then the problem can be stated mathematically as:

$$\frac{\partial^2 T}{\partial x^{*2}} = \frac{1}{\alpha}\frac{\partial T}{\partial t^*}, \tag{1}$$

with the following initial and boundary conditions:

1. $T(x^*, 0) = 0$ (2a)

2. $\dfrac{\partial T}{\partial x}(0, t^*) = 0$ (2b)

3. $T(L, t^*) = T_s(t^*) = ?$ (2c)

Introducing the dimensionless independent variables,

$$x = x^*/L \tag{3}$$

$$t = \alpha t^*/L^2. \tag{4}$$

Equations (1) and (2) become:

$$\frac{\partial^2 T}{\partial x^2} = \frac{\partial T}{\partial t}, \tag{5}$$

with

1. $T(x, 0) = 0$ (6a)

2. $\dfrac{\partial T}{\partial x}(0, t) = 0$ (6b)

3. $T(1, t) = T_s(t) = ?$ (6c)

If, in addition, the temperature is approximately known at interior points at discrete times, i.e.

$$T(\varepsilon_i, \tau_i) \doteq \gamma_i, \quad i = 1,2,\ldots,N, \tag{6d}$$

with errors $\Delta\gamma_i$, then the surface temperature history, $T_s(t)$, can be estimated. The estimation improves as N increases and $\Delta\gamma_i$ decreases.

For a known $T_s(t)$ the direct solution of equations (5) and (6) can be given by Duhamel's formula [26]:

$$T(x, t) = \int_0^t T_s(\lambda)\frac{\partial V}{\partial t}(x, t-\lambda)\,d\lambda, \tag{7}$$

where V is the solution to the supplementary problem

$$\frac{\partial^2 V}{\partial x^2} = \frac{\partial V}{\partial t}, \tag{8}$$

with

1. $V(x, 0) = 0$ (9a)

2. $\dfrac{\partial V}{\partial x}(0, t) = 0$ (9b)

3. $V(1, t) = \begin{cases} 0, & t < 0 \\ 1, & t > 0. \end{cases}$ (9c)

For the present case V can be expressed either as an infinite series of cosines or an infinite series of error functions. The latter method is chosen for its better convergence at small times. The solution for V is given by [26]:

$$V(x, t) = \sum_{n=0}^{\infty}(-1)^n \times\left[\operatorname{erfc}\left(\frac{B_n - x}{2\sqrt{t}}\right) + \operatorname{erfc}\left(\frac{B_n + x}{2\sqrt{t}}\right)\right], \tag{10}$$

where

$$B_n = 2n + 1. \tag{11}$$

Thus

$$\frac{\partial V}{\partial t}(x, t-\lambda) = \frac{1}{2\sqrt{\pi}}\sum_{n=0}^{\infty}\frac{(-1)^n}{(t-\lambda)^{3/2}} \times\left[(B_n - x)\,e^{-(B_n - x)^2/4(t-\lambda)} + (B_n + x)\,e^{-(B_n - x)^2/4(t-\lambda)}\right]. \tag{12}$$

If $T_s(\lambda)$ is unknown but $T(x, t)$ is known to within some measurement error at the points ε_i, τ_i, $i =$

$1, 2, \ldots, N$, then equation (7) can be written as

$$\gamma_i \doteq T(\varepsilon_i, \tau_i) = \int_0^{\tau_i} T_s(\lambda) \frac{\partial V}{\partial t}(\varepsilon_i, \tau_i - \lambda)\, d\lambda, \quad i = 1, 2, \ldots, N. \tag{13}$$

For convenience let

$$K(\varepsilon_i, \tau_i, \lambda) = \begin{cases} \dfrac{\partial V}{\partial t}(\varepsilon_i, \tau_i - \lambda), & \lambda \leqslant \tau_i, \\ 0, & \lambda > \tau_i, \end{cases} \tag{14}$$

where $K(\varepsilon_i, \tau_i, \lambda)$ is an integrating kernel. Equation (13) can be written as

$$\gamma_i \doteq \int_0^{\tau_N} T_s(\lambda) K(\varepsilon_i, \tau_i, \lambda)\, d\lambda, \quad i = 1, 2, \ldots, N, \tag{15}$$

where τ_N is the time of the last known interior temperature measurement γ_N. The problem of evaluating $T_s(\lambda)$ from discrete and noisy empirical data γ_i is reduced to finding $T_s(\lambda)$ from the simultaneous integral equations (15).

Solution of the simultaneous integral equations

Although the inverse problem posed is very specific (equations (5) and (6) with interior conditions (6d)), any inverse conduction problem expressible in the form of equation (15) can be evaluated using the following technique. Consider the set of integral equations of the form:

$$\gamma_i \doteq \int_0^{\tau_N} T_s(\lambda) K(\mathbf{r}_i, \tau_i, \lambda)\, d\lambda, \quad i = 1, 2, \ldots, N, \tag{16}$$

where $\mathbf{r}_i$ is the position vector of the measurement γ_i (not necessarily one dimensional). We wish to find a $T_s(\lambda)$ over the interval $0 \leqslant t \leqslant \tau_N$ that best satisfies equation (16) at the measurements $\gamma_i, i = 1, 2, \ldots, N$. Consider the analogy between equation (16) and the inverse problem in linear algebra. Write equation (16) as follows:

$$\gamma_i \doteq \lim_{M \to \infty} \sum_{j=1}^{M} T_s(\lambda_j)[K(\mathbf{r}_i, \tau_i, \lambda_j)\Delta\lambda], \quad i = 1, 2, \ldots, N, \tag{17}$$

where the interval $(0, \tau_N)$ is divided into M equal segments, $\Delta\lambda$, and λ_j represents the value of λ at the midpoint of the jth segment. Thus

$$\Delta\lambda = \tau_M / M. \tag{18}$$

Equation (17) represents a system of N equations with M unknowns $T_s(\lambda_j)$ with $M \to \infty$. Expressing equation (17) in matrix form gives:

$$\gamma \doteq \bar{\mathbf{A}} \mathbf{T}_s, \tag{19}$$

where

$$\gamma = [\gamma_1, \gamma_2, \ldots, \gamma_N]^T \tag{20}$$

$$\mathbf{T}_s = [T_s(\lambda_1), T_s(\lambda_2), \ldots, T_s(\lambda_M)]^T \tag{21}$$

$$\bar{\mathbf{A}} = \begin{bmatrix} K(\mathbf{r}_1, \tau_1, \lambda_1)\Delta\lambda & K(\mathbf{r}_1, \tau_1, \lambda_2)\Delta\lambda & \ldots & K(\mathbf{r}_1, \tau_1, \lambda_M)\Delta\lambda \\ K(\mathbf{r}_2, \tau_2, \lambda_1)\Delta\lambda & & & \vdots \\ \vdots & & & \\ K(\mathbf{r}_N, \tau_N, \lambda_1)\Delta\lambda & \ldots & & K(\mathbf{r}_N, \tau_N, \lambda_M)\Delta\lambda \end{bmatrix}.$$

If $\bar{\mathbf{A}}$ was square with rank equal to its order then a unique inverse would exist;

$$\mathbf{T}_s \doteq \bar{\mathbf{A}}^{-1} \gamma, \tag{23}$$

with the error in T_s of

$$\Delta\mathbf{T}_s = \bar{\mathbf{A}}^{-1} \Delta\gamma, \tag{24}$$

where

$$\Delta\gamma = [\Delta\gamma_1, \Delta\gamma_2, \ldots, \Delta\gamma_N]^T \tag{25}$$

$$\Delta\mathbf{T}_s = [\Delta T_{s_1}, \Delta T_{s_2}, \ldots, \Delta T_{s_N}]^T. \tag{26}$$

For the present problem $\bar{\mathbf{A}}$ is not square and only a pseudo-inverse [27] $\bar{\mathbf{B}}$ can be found with the properties

$$\bar{\mathbf{A}}\bar{\mathbf{B}} = \bar{\mathbf{I}} \quad (\bar{\mathbf{I}} \text{ the identity matrix}), \tag{27}$$

but

$$\bar{\mathbf{B}}\bar{\mathbf{A}} \neq \bar{\mathbf{I}}, \tag{28}$$

where $\bar{\mathbf{B}}$ is chosen such that $\bar{\mathbf{B}}\bar{\mathbf{A}}$ approximates $\bar{\mathbf{I}}$ as well as possible. The approximate solution, $\hat{\mathbf{T}}_s$, to equation (19) will then be:

$$\hat{\mathbf{T}}_s = \mathbf{B}\gamma, \tag{29}$$

and from equation (19)

$$\hat{\mathbf{T}}_s = \bar{\mathbf{B}}\bar{\mathbf{A}}\mathbf{T}_s. \tag{30}$$

Thus, the prediction $\hat{T}_{s_K}$ is a weighted average of the actual surface temperatures $T_{s_j}, j = 1, 2, \ldots, M$, where the weighted function is given by the kth row of $\bar{\mathbf{B}}\bar{\mathbf{A}}$.

Dealing with $N \times M$ matrices with $M \to \infty$ is unrealistic. However, an important concept surfaces from the linear algebra analogy. Equation (29) states that $\mathbf{T}_s$ can be approximated by $\bar{\mathbf{B}}\gamma$ and each element in $\mathbf{T}_s$ is approximated by a linear combination of the measurements γ_i. If the measurements were exact and if an infinity of independent measurements were available then a $\bar{\mathbf{B}}$ would exist such that

$$\bar{\mathbf{B}}\bar{\mathbf{A}} = \bar{\mathbf{I}}, \tag{31}$$

and equation (30) would become:

$$\hat{\mathbf{T}}_s = \mathbf{T}_s. \tag{32}$$

In view of the above discussion, let T_s at some time t be approximated by a linear combination of the measurements γ_i, i.e.

$$T_s(t) \doteq \sum_{i=1}^{N} a_i \gamma_i = \hat{T}_s(t). \tag{33}$$

Using equation (16) in equation (33) gives:

$$\hat{T}_s(t) \doteq \sum_{i=1}^{N} a_i \int_0^{\tau_N} T_s(\lambda) K(\mathbf{r}_i, \tau_i, \lambda) \mathrm{d}\lambda, \quad (34)$$

or

$$\hat{T}_s(t) \doteq \int_0^{\tau_N} T_s(\lambda) \left[\sum_{i=1}^{N} a_i K(\mathbf{r}_i, \tau_i, \lambda) \mathrm{d}\lambda \right]. \quad (35)$$

In analogy with equation (31), if the a_i can be chosen such that

$$D(\lambda) = \sum_{i=1}^{N} a_i K(\mathbf{r}_i, \tau_i, \lambda), \quad (36)$$

represents a Delta–Dirac function $\delta(t-\lambda)$, then

$$\hat{T}_s(t) \doteq T_s(t). \quad (37)$$

Since an exact representation for a finite number of measurements, N, is not possible, the a_i are chosen such that $D(\lambda)$ approximates $\delta(t-\lambda)$ as well as possible. Using equation (36) in equation (35) gives

$$\hat{T}_s(t) = \int_0^{\tau_N} T_s(\lambda) D(\lambda) \mathrm{d}\lambda. \quad (38)$$

Thus, $D(\lambda)$ is an averaging kernel and the resulting predictions for the surface condition, $\hat{T}_s(t)$, will be a weighted average of the actual surface condition $T_s(t)$. If $D(\lambda)$ has an infinitesimal width and is centered at $\lambda = t$, then $T_s(t)$ is resolved totally by $\hat{T}_s(t)$. Given the kernels $K(\mathbf{r}_i, \tau_i, \lambda)$ of equation (16), if the a_i of equation (36) can be chosen such that $D(\lambda)$ best approximates a Delta–Dirac function at time t, then by equation (33), the approximate surface condition is given by:

$$\hat{T}_s(t) = \sum_{i=1}^{N} a_i \gamma_i. \quad (33)$$

Choosing the coefficients a_i

In evaluating the coefficients a_i of equation (36), a measure of closeness to the Delta–Dirac function is needed. One possibility is to minimize the square of the difference between $D(\lambda)$ of equation (36) and the Delta–Dirac function. In this case, the parameter I as defined below must be minimized by choosing the appropriate a_i for each time t.

$$I = \int_0^{\tau_N} [\delta(t-\lambda) - D(\lambda)]^2 \mathrm{d}\lambda. \quad (39)$$

Minimizing equation (39) does not necessarily give the optimum result since all points in the interval $0 \leqslant \lambda \leqslant \tau_N$ are weighted equally. Backus and Gilbert [25] suggest the following criteria:

$$I = \int_0^{\tau_N} (t-\lambda)^2 D^2(\lambda) \mathrm{d}\lambda, \quad (40)$$

with the additional constraint that $D(\lambda)$ be unimodular, i.e.

$$\int_0^{\tau_N} D(\lambda) \mathrm{d}\lambda = 1. \quad (41)$$

By minimizing equation (40) with the constraint of equation (41), a narrower $D(\lambda)$ will be found than would be possible by the minimization of equation (39) due to the weight function $(t-\lambda)^2$. In view of equation (40), the spread of $D(\lambda)$ around t can be defined as:

$$s = 30 \int_0^{\tau_N} (t-\lambda)^2 D^2(\lambda) \mathrm{d}\lambda, \quad (42)$$

where the quantity 30 is a normalization constant chosen so that the spread, s, of a $D(\lambda)$ of the form of a triangular wave as shown in Fig. 2 will be equal to the width of the wave. The predictions $\hat{T}_s(t)$, equation (38), will be a weighted average of the actual surface temperature over a time interval represented by the spread of the Delta–Dirac approximating function $D(\lambda)$. The spread, therefore, quantifies a minimum time scale (temporal resolution) over which $T_s(t)$ can be determined for a given set of measurement times and positions.

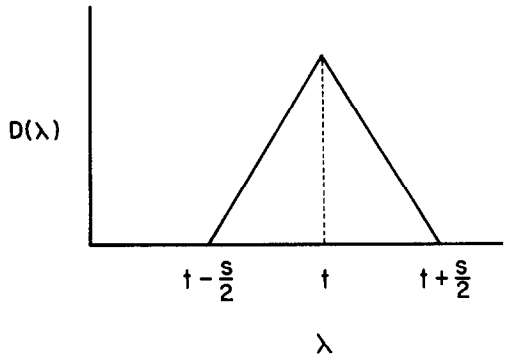

FIG. 2. Idealized form of $D(\lambda)$.

Using equation (36) in equations (41) and (42) gives:

$$\mathbf{u}^T \mathbf{a} = 1 \quad (43)$$

$$s = \mathbf{a}^T \bar{\mathbf{S}} \mathbf{a}, \quad (44)$$

with

$$\mathbf{a} = [a_1, a_2, \ldots, a_N]^T \quad (45)$$

$$\mathbf{u} = [u_1, u_2, \ldots, u_N]^T, \quad (46)$$

where

$$u_i = \int_0^{\tau_N} K(\mathbf{r}_i, \tau_i, \lambda) \mathrm{d}\lambda. \quad (47)$$

Also

$$\bar{\mathbf{S}} = \begin{bmatrix} S_{11} & S_{12} & \cdots & S_{1N} \\ \vdots & & & \\ S_{N1} & \cdots & \cdots & S_{NN} \end{bmatrix}, \quad (48)$$

where

$$S_{ij} = 30 \int_0^{\tau_N} (t-\lambda)^2 K(\mathbf{r}_i, \tau_i, \lambda) K(\mathbf{r}_j, \tau_j, \lambda) \mathrm{d}\lambda. \quad (49)$$

Once the $\mathbf{a}$ vector is chosen, $\hat{T}_s(t)$ is given by:

$$\hat{T}_s(t) = \mathbf{a}^T \gamma, \quad (50)$$

where

$$Y = [Y_1, Y_2, \cdots, Y_N]^T, \tag{51}$$

and the error in $\hat{T}_s(t)$ due to errors in Y is

$$\Delta\hat{T}_s(t) = \mathbf{a}^T\Delta Y. \tag{52}$$

If the measurement errors, ΔY_i, have a probability distribution whose means are zero and whose second moments exist then we can let the square of the error be denoted by ε^2; thus:

$$\varepsilon^2 = (\Delta\hat{T}_s(t))^2 = \mathbf{a}^T\bar{\mathbf{E}}\mathbf{a} \tag{53}$$

where $\bar{\mathbf{E}}$ is the covariance matrix.

$$\bar{\mathbf{E}} = \begin{bmatrix} \Delta Y_1\Delta Y_1 & \Delta Y_1\Delta Y_2 & \Delta Y_1\Delta Y_N \\ \Delta Y_2\Delta Y_1 & & \vdots \\ \vdots & & \vdots \\ \Delta Y_N\Delta Y_1 & \cdots & \Delta Y_N\Delta Y_N \end{bmatrix}. \tag{54}$$

Backus and Gilbert [25] solved equations (43) (44), and (53) and found that as the spread, s, decreased, the error, ε, increased. Physically, this means that as the temporal resolution of the surface conditions increases, the error in the predicted surface conditions increased. By choosing an $\mathbf{a}$ such that the spread, s, is not optimized, a smaller error, ε, can be obtained. A compromise between resolving power and accuracy must be reached. Define

$$\bar{\mathbf{W}} = (1-\beta)\bar{\mathbf{S}} + \beta\bar{\mathbf{E}}. \tag{55}$$

Then $\mathbf{a}^T\bar{\mathbf{W}}\mathbf{a}$ becomes:

$$w = \mathbf{a}^T\bar{\mathbf{W}}\mathbf{a} = (1-\beta)s + \beta\varepsilon^2. \tag{56}$$

By varying β between 0 and 1 and minimizing w with respect to $\mathbf{a}$, the trade-offs between resolving power, s, and accuracy, ε, can be studied. The optimum solution of equation (56) for a given β, with the constraint of equation (43) is [25]:

$$a(\beta) = \frac{\bar{\mathbf{W}}^{-1}\mathbf{u}}{\mathbf{u}^T\bar{\mathbf{W}}^{-1}\mathbf{u}}. \tag{57}$$

Once the $\mathbf{a}$ vector is found from equation (57), the spread, error, and surface condition at time t can be given as:

$$s = \mathbf{a}^T\bar{\mathbf{S}}\mathbf{a} \tag{44}$$

$$\varepsilon^2 = \mathbf{a}^T\bar{\mathbf{E}}\mathbf{a} \tag{53}$$

$$\hat{T}_s(t) = \mathbf{a}^T Y. \tag{50}$$

RESULTS

Error free data

Although all experiments have error, studying the effects of errorless measurements can give insight into the maximum possible resolution of surface conditions available from the measurements. The only error introduced into the problem is the error due to computer roundoff. To illustrate the power of the method, the method was implemented on an IBM 360 using single precision arithmetic.

As an initial example, consider measurements taken at $x = 0.5$ at equally spaced times. Using the time and location of each measurement (the actual value of the measurement is not needed) graphs for spread, s, vs time were generated as illustrated in Fig. 3. Three cases were considered. The first case consisted of 20 measurements taken at 20 equally spaced times ($\Delta t = 0.1$) in the interval $0 < t \leqslant 2.0$. The values of spread of the surface predictions were generated for the same discrete times. The figure illustrates that the spread is a weak function of time over most times of interest. Around $t = 2$, however, there is a sharp rise in the spread reflecting the inability of the internal measurements taken over the interval $0 < t \leqslant 2.0$ to sense changes in the surface temperature at $t = 2$.

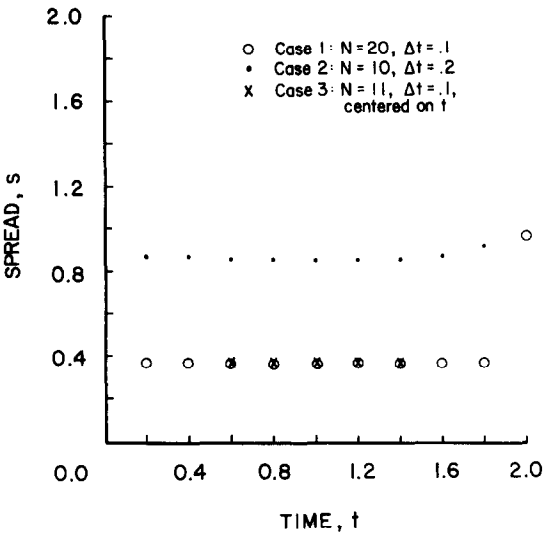

FIG. 3. Spread vs time for error-free data.

The second case considered consisted of 10 equally spaced measurements at $x = 0.5$ with $\Delta t = 0.2$ over the interval $0 < t \leqslant 2.0$. As in the first case, the spread increases rapidly near $t = 2$, the end of the sampling period. The spread also increased significantly as a result of the fewer measurements.

The third case illustrates that the surface temperature history can be represented by using 11 measurements, 5 on each side of the time of interest and 1 at the time of interest, with approximately the same spread as using all 20 measurements distributed over the entire interval. The surface temperature histories are thus largely a function of measurements made during a $\Delta t = 1$ interval surrounding the time of interest. Table 1 further illustrates the preceding point; tabulated are the $\mathbf{a}$ vectors at $t = 1$ for cases 1 and 3. Since $\hat{T}_s(1) = \mathbf{a}^T Y$ then $\hat{T}_s$ depends mostly on the measurements made in the interval around $t = 1.0$. As shown in Table 1, the measurement taken at $t = 1.1$ has the largest weight indicating that of all the measurements, the measurement at $t = 1.1$ best reflects the conditions on the surface at $t = 1.0$.

In view of the above results, an additional plot of spread vs time for $0.9 \leqslant t \leqslant 1.1$ was made in the hope that at some time within the interval the spread is a minimum. Eleven measurement times were used with $\Delta t = 0.1$, centered at $t = 1.0$. The results, as

Table 1. The coefficient vector **a** for $t = 1$ for cases 1 and 3

Time of measurement	**a**, Case 1	**a**, Case 3
0.1	−0.0002159	
0.2	−0.0008528	
0.3	−0.0022914	
0.4	−0.0056048	
0.5	−0.0132885	−0.0185589
0.6	−0.0313024	−0.0326914
0.7	−0.073896	−0.075551
0.8	−0.169285	−0.171887
0.9	−0.516504	−0.523498
1.0	−0.089510	−0.092030
1.1	1.664683	1.687145
1.2	0.140083	0.142325
1.3	0.0463462	0.0467732
1.4	0.0210975	0.0228954
1.5	0.0117186	0.0208453
1.6	0.0073413	
1.7	0.0050258	
1.8	0.0037523	
1.9	0.0030969	
2.0	0.0045095	

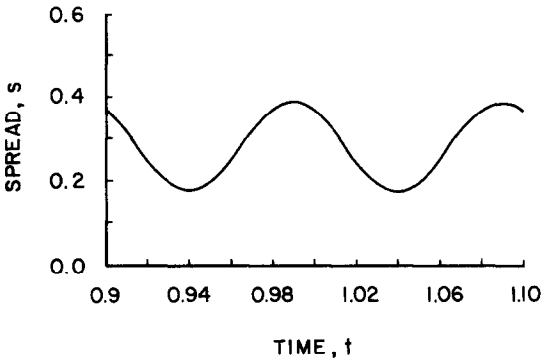

FIG. 4. Spread vs time for error-free data; $0.9 \leqslant t \leqslant 1.1$

shown in Fig. 4, illustrate a periodic behavior. The spread of a surface temperature prediction at $t = 1.04$ is less than one-half the spread for $t = 0.99$. Tabulated in Table 2 are the a_i coefficients for the times corresponding to the peaks and troughs of the spread curve of Fig. 4. The contents of Table 2 indicate that the temperature at $t = 0.94$ depends mostly (see equation (50)) on the measurement made at $t = 1.0$. The predicted surface temperature responses at $t = 0.99$, 1.04, and 1.09 depend mostly on the measurements at $t_i = 1.1$, 1.1, 1.2, respectively. The above results reflect the time lag in the response of an interior point to a surface condition.

In the previous results presented, no mention of the magnitude of the measurements were made. The previous results do not depend on the magnitude of the measurements, but only upon their time and location. After the analysis as presented is complete and the **a** vector found for each time of interest, the experiment can be run for any surface temperature history, $T_s(t)$, with measurements, Y_i, made at times t_i. The surface temperature histories can then be analysed by use of equation (50) for each **a**:

$$\hat{T}_s(t) = \mathbf{a}^t Y. \tag{50}$$

As an example, consider the surface temperature history given by the solid line of Fig. 5. Using the interior conditions at $x = 0.5$ generated by the exact solution (see [10]) of the corresponding forward problem with the surface conditions indicated, the corresponding approximate surface temperature history was evaluated by the use of equation (50) and the **a** vectors calculated from the previous results.

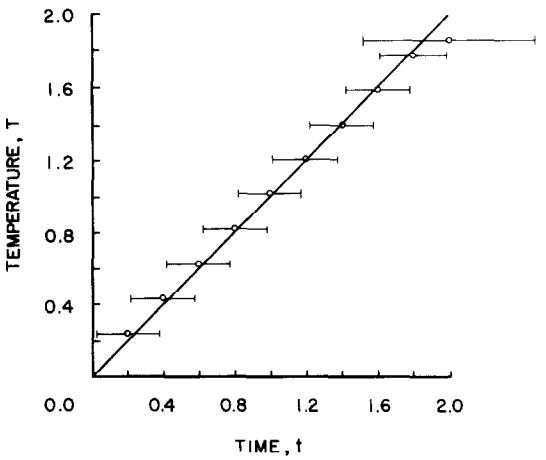

FIG. 5. Actual and predicted surface temperatures as a function of time. The horizontal bars represent spread. Number of measurements = 20.

Table 2. The coefficient vector as a function of time

Time of measurement	**a**, $t = 0.94$	**a**, $t = 0.99$	**a**, $t = 1.04$	**a**, $t = 1.09$
0.5	−0.02795	−0.02159	−0.01121	−0.00892
0.6	−0.05190	−0.03798	−0.02099	−0.01614
0.7	−0.12711	−0.08792	−0.05086	−0.03729
0.8	−0.29730	−0.19755	−0.12628	−0.08763
0.9	−1.38934	−0.67391	−0.29680	−0.19806
1.0	2.70276	0.54247	−1.38978	−0.67669
1.1	0.13458	1.26157	2.70593	0.54668
1.2	0.03266	0.13201	0.13423	1.26674
1.3	0.01378	0.04635	0.03262	0.13326
1.4	0.00764	0.02285	0.01429	0.04796
1.5	0.00774	0.02121	0.01199	0.03504

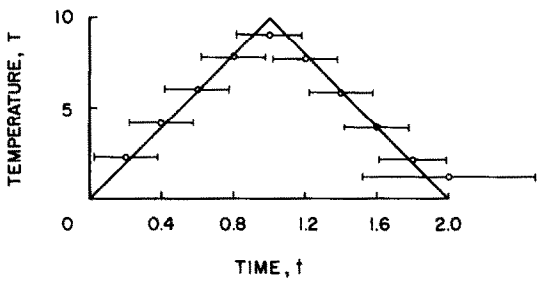

FIG. 6. Actual and predicted surface temperatures as a function of time. The horizontal bars represent spread. Number of measurements = 20.

Also plotted for each prediction is the spread represented by a horizontal line "centered" on the time of the corresponding prediction. In all cases, the actual surface temperature lies well within the spread of the corresponding surface temperature.

Illustrated in Fig. 6 is a comparison between predicted and actual surface temperature histories for an alternate $T_s(t)$. The errorless (within single precision machine accuracy) experimental internal measurements were simulated by using the following exact solution for the forward heat conduction problem with the surface condition of Fig. 6. Double precision arithmetic was used.

$$T(x,t) = 10t + 20\sum_{n=1}^{\infty}\frac{(-1)^{n-1}}{B_n^3} \times (1-e^{-B_n^2 t})\cos(B_n x),\ 0 < t \leqslant 1 \quad (58)$$

$$T(x,t) = 10t + 20\sum_{n=1}^{\infty}\frac{(-1)^{n-1}}{B_n^3} \times (1+e^{-B_n^2 t} - 2e^{-B_n^2(t-1)})\cos(B_n x),\ 1 < t \leqslant 2, \quad (59)$$

where

$$B_n = \frac{2n-1}{2}\pi. \quad (60)$$

As in the previous case $x = 0.5$. Truncating the series after 1200 terms gave simulated measurements accurate to 6 significant figures. All predictions lie within the spread of the corresponding surface conditions. The prediction at $t = 1$ is of particular interest. Equation (38) states that each prediction is a weighted average of the actual surface conditions. Thus, the prediction at $t = 1$ is in fact a weighted average of the actual surface conditions over an interval width of approximately $\Delta t = 0.36$. This indicates that for the present theory the prediction at such a peak (at $t = 1$) must always be less than the actual surface temperature at the peak for errorless data.

As a result of one of the reviewers' suggestions, the method was applied to errorless measurements taken at very small time steps, Δt. The results indicated that as Δt decreases below 0.5, no significant improvement in spread is obtained. Decreasing Δt only results in the need to invert larger matrices for which each additional measurement provides less additional information. Therefore, decreasing Δt eventually leads to algorithmetically singular matrices. Using double precision computation would extend the lower limit of Δt, but no additional information would be gained since the spread would not significantly improve.

Data with error

By appropriately choosing a β for equation (56), a compromise between spread (resolving power) and accuracy can be attained for measurement data with errors. To illustrate this point, the present method was applied to the numerically generated measurements used in the previous cases. To simulate experimental error a normal independent distributed random error with a mean of 0 and a variance chosen so that the bound ± 0.02 (1% of $T_s(2)$) represents the 99% confidence level on the error, was added to the measurement data. In view of the results of the previous section (see Fig. 3) the surface temperature histories were analyzed by using the 11 measurement data points closest in time ($\Delta t = 0.1$) to the surface temperature prediction time. In addition (see Fig. 4), the prediction times were taken as 0.14, 0.34, 0.54, ..., 1.94 to minimize spread. Illustrated in Fig. 7 is a plot of spread vs error (also 99% confidence level) for $t = 0.14$, 0.94, and 1.74. It is interesting to note that for prediction error greater than the measurement error, the three cases nearly coincide and are only weak functions of the error. To

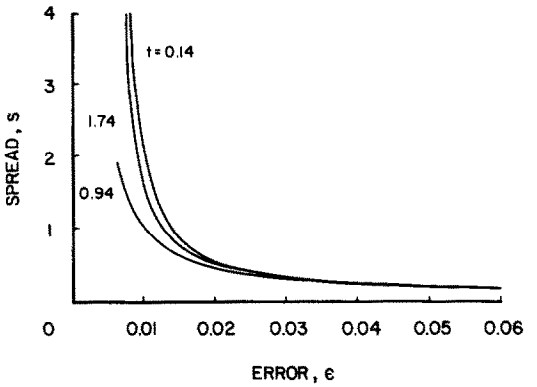

FIG. 7. Spread as a function of error for $t = 0.14$, 0.94, 1.74.

give predictions with error on the order of the measurement error without sacrificing spread, a value of β was chosen such that the magnitude of the error was in the interval (0.03, 0.04) over the entire range of interest. Figure 8 illustrates the results of such a choice of β. The inclined solid line represents the actual surface temperature, and the points represent the predictions. The horizontal and vertical bars on each point represent the spread and error for each prediction. The spread bars are centered on the prediction times strictly for convenience. The centers of the actual weighting functions ($D(\lambda)$ of equation (38)), however, are not necessarily at the prediction times. The result of each prediction is a weighted

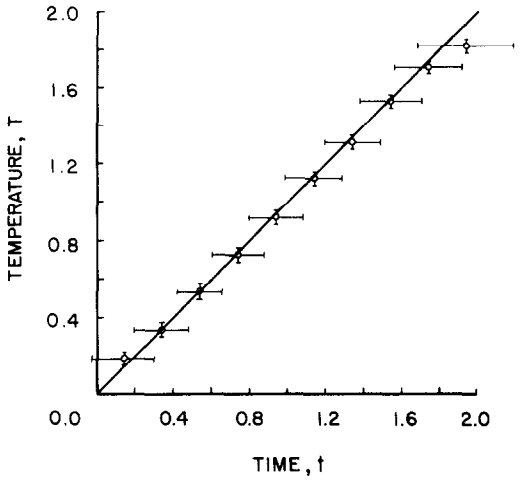

FIG. 8. Actual and predicted surface temperatures as a function of time for measurement data with 0.02 error. The horizontal and vertical bars represent spread and error.

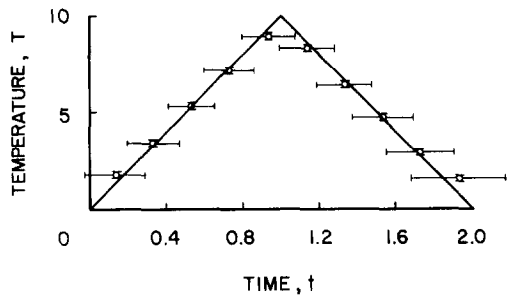

FIG. 9. Actual and predicted surface temperatures as a function of time for measurement data with ± 0.1 error. The horizontal and vertical bars represent spread and error.

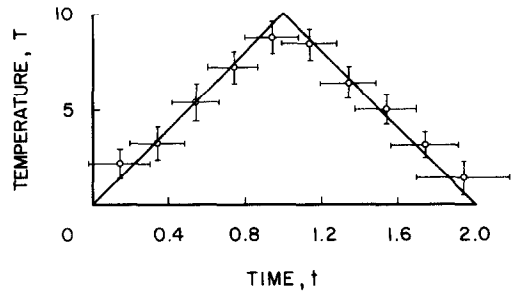

FIG. 10. Actual and predicted surface temperatures as a function of time for measurement data with ± 0.5 error. The horizontal and vertical bars represent spread and error.

average, within the vertical error bounds, of the actual surface temperature history over a time spread represented by the horizontal bars.

Figures 9 and 10 show predictions for the alternate surface temperature history. In the case of Fig. 9, a ± 0.1 error (1% ot $T_s(1)$) was added to the simulated measurements while in the case of Fig. 10, a ± 0.5 error (5% of $T_s(1)$) was added. In both cases the predictions are within the bounds illustrated and no instability (which occurs in some other methods) is apparent.

CONCLUSIONS

A method has been presented that enables the quantitative evaluation of the resolving power and accuracy of surface temperature predictions generated from inaccurate and discrete interior measurements. While the method was only demonstrated for a simple geometry $(1-D)$, it can be adapted to more general geometries by choosing the appropriate definition for spread (see [19]). The method can also be extended to handle surface flux evaluations as will be demonstrated in a later paper.

REFERENCES

1. G. Stolz, Jr., Numerical solutions to an inverse problem of heat conduction for simple shapes, *J. Heat Transfer, Trans. ASME, Series C.* **82**, 20–26 (1960).
2. D. R. Hartree, *Numerical Analysis*, Oxford University Press, London (1952).
3. J. V. Beck and H. Wolf, The non-linear inverse heat conduction problem, ASME Paper No. 65-HT, 40 (1965).
4. T. P. Fidelle and G. E. Zinsmeister, A semi-discrete approximate solution of the inverse problem of transient heat conduction, ASME Paper No. 68-WA/HT-26 (1968).
5. J. V. Beck, Non-linear estimation applied to the non-linear inverse heat conduction problem, *Int. J. Heat Mass Transfer* **13**, 703–716 (1970).
6. N. D'Souza, Numerical solution of one-dimensional inverse transient heat conduction by finite difference method, ASME Paper No. 75-WA/HT-81 (1975).
7. P. S. Hore, G. W. Krutz and R. J. Schoenhals, Application of the finite element method to the inverse heat conduction problem, ASME Paper No. 77-WA/TM-4 (1977).
8. I. Frank, An application of least squares method to the solution of the inverse problem of heat conduction, *J. Heat Transfer* **85C**, 378–379 (1963).
9. G. P. Mulholland, B. P. Gupta and R. L. San Martin, Inverse problem of heat conduction in composite media, ASME Paper No. 75-WA/HT-83 (1975).
10. R. G. Arledge and A. Haji-Sheikh, An iterative approach to the solution of inverse heat conduction problems, ASME Paper No. 77-WA/TM-2 (1977).
11. R. Bellman and J. M. Richardson, A note on an inverse problem in mathematical physics, *Q. Appl. Math.* **19**, 269–271 (1961).
12. S. D. Williams and D. M. Curry, Surface heat flux determination – an analytical and experimental study using a single-embedded thermocouple, NASA TM-58204 (1977).
13. E. M. Sparrow, A. Haji-Sheikh and T. S. Lundgren, The inverse problem in transient heat conduction, *J. appl. Mech.* **86E**, 369–375 (1964).
14. L. I. Deverall and R. S. Channapragada, A new integral equation for heat flux in inverse heat conduction, *J. Heat Transfer* **88C**, 327–328 (1966).
15. O. R. Burggraf, An exact solution of the inverse problem in heat conduction theory and applications, *J. Heat Transfer* **86C**, 373–382 (1964).
16. A. V. Masket and A. C. Vastano, Interior value problems of mathematical physics. Part 1. Wave propagation, *Am. J. Phys.* **30**, 687–696 (1962).
17. A. V. Kover'yanov, Inverse problem of nonsteady state thermal conductivity, *High temperature* **5**, 121–127 (1967).
18. I. C. Heron, An evaluation of errors that occur in the solution of the inverse heating problem for flat plates and hemispherical shells, Australian Defense Scientific Service, Technical Note HSA 188 (November 1970).

19. L. D. Kalinnikov, Solution of the inverse heat conduction problem in the case of a piecewise linear approximation of the boundary conditions, *High Temperature* **9**, 906–910 (1972).
20. J. V. Beck, Thermocouple temperature disturbance in low conductivity materials, *J. Heat Transfer* **84C**, 124–132 (1962).
21. J. V. Beck, Calculation of thermal diffusivity from temperature measurements, *J. Heat Transfer* **85C**, 181–182 (1963).
22. J. V. Beck, Determination of undisturbed temperatures from thermocouple measurements using correction kernels, *Nucl. Engng Design* **7**, 9–12 (1968).
23. J. V. Beck, Sensitivity coefficients utilized in non-linear estimation with small parameters in a heat transfer problem, ASME Paper No. 69-WA/Aut.-4 (1969).
24. J. V. Beck and S. Al-Araji, Investigation of a new simple transient method of thermal property measurement, *J. Heat Transfer* **96**, 59–64 (1974).
25. B. Backus and F. Gilbert, Uniqueness in the inversion in inaccurate gross earth data, *Phil. Trans. R. Soc., Lond.* **266**, 123–192 (1970).
26. R. V. Churchill, *Operational Mathematics*, McGraw-Hill, New York (1972).
27. C. Lanczos, *Linear Differential Operators*, D. Van Nostrand, Princeton, New Jersey (1964).

PRECISION ET POUVOIR DE RESOLUTION D'UNE THEORIE INVERSE DE LA CONDUCTION THERMIQUE APPLIQUE A DES MESURES DISCRETES ET IMPRECISES

Résumé—Le problème inverse de la conduction thermique est défini comme correspondant à des conditions internes données l'inconnue étant une condition de surface. Dans ce travail, l'histoire de la température de surface d'un mur infini est évaluée à partir de mesures internes, discrètes et imprécises. La méthode de Backus et Gilbert est utilisée pour déterminer le pouvoir de résolution des mesures et la précision des calculs de la température de surface. On illustre la distinction à faire entre le pouvoir de résolution et la précision.

DIE GENAUIGKEIT UND DAS AUFLÖSUNGSVERMÖGEN EINER EINDIMENSIONALEN INSTATIONÄREN INVERSEN WÄRMELEITUNGSTHEORIE BEI IHRER ANWENDUNG AUF DISKRETE UND UNGENAUE MESSUNGEN

Zusammenfassung—Das inverse Wärmeleitungsproblem ist definiert als die Aufgabe, bei der innere Bedingungen gegeben sind und die gesuchte Größe eine Oberflächenbedingung ist. In der vorliegenden Arbeit werden zeitlich zurückliegende Temperaturverläufe an der Oberfläche einer unendlichen Platte unter Verwendung diskreter, ungenauer innerer Messungen ermittelt. Die Methode von Backus und Gilbert wird verwendet, um das Auflösungsvermögen der Messungen und die Genauigkeit der resultierenden Oberflächentemperaturen zu bestimmen. Die Zusammenhänge zwischen Auflösungsvermögen und Genauigkeit werden erläutert.

ТОЧНОСТЬ И РАЗРЕШИМОСТЬ ОДНОМЕРНОЙ НЕСТАЦИОНАРНОЙ ОБРАТНОЙ ТЕОРИИ ТЕПЛОПРОВОДНОСТИ ПРИМЕНИТЕЛЬНО К ДИСКРЕТНЫМ И ПРИБЛИЖЕННЫМ ИЗМЕРЕНИЯМ

Аннотация — Обратной задачей теплопроводности является такая задача, в которой внутренние условия заданы, а искомая величина представляет собой условие на поверхности. В настоящей работе изменение температуры поверхности бесконечной плиты определяется с помощью дискретных и приближенных измерений внутренних величин. Разрешающая способность измерений и точность результатов измерений температуры поверхности определяется методом Бэкуса–Джильберта. Показана взаимосвязь между разрешимостью и точностью.